Implementation of a Non-codebook Based MU-MIMO System for TDD LTE-Advanced

Daejin KIM, Sangwook HAN, Yong JIN, Heungseop AHN and Seungwon CHOI
Dept. of Electronic and Computer Engineering
Hanyang University
Seoul, Korea
Email: {kdj317, ssssang3234, kimyong84, ahs90, choi}@dsplab.hanyang.ac.kr

***Abstract*—This paper presents a non-codebook based Multiple User Multiple Input Multiple Output (MU-MIMO) test-bed system for Time Division Duplexing (TDD) Long Term Evolution-Advanced (LTE-A), which has been implemented for verifying the performance of a dynamic precoding procedure. Using the parameter of propagation path gain, the proposed MU-MIMO system can adaptively switch the precoder to guarantee that the upper bound BER is maintained with a minimum computational burden.**

Keywords—LTE-A, MU-MIMO, Dynamic precoding

I. INTRODUCTION

The Single-User MIMO (SU-MIMO) system considers a single multi-antenna transmitter communicating with a single multi-antenna receiver. In contrast, the MU-MIMO system allows multiple independent radio terminals, each of which has one or multiple antennas that communicate with a given access point in such a way that each radio terminal can fully utilize all the spectral resources simultaneously [1, 2]. Due to the fact that the spectral resources are shared in all the terminals, the MU-MIMO system must employ a proper procedure to resolve the problem of interference among the signals transmitted from an access point to the multiple terminals in the same frequency band at the same time. This is why the problem of designing an MU-MIMO system often includes a user selection procedure [3-5] for selecting a set of user terminals for which the corresponding channels are close to orthogonal to one another. This criterion consequently guarantees that the interference among the selected terminals is at a minimum. In addition to user selection, a counter-measuring technology to the intrinsic problem of MU-MIMO resulting from the interference among terminals, MU-MIMO must include a precoding procedure at the transmitting access point as a methodology of space-division multiple access [6, 7].

In an MU-MIMO system, which in general has to include a precoding procedure as mentioned above, the User Equipment (UE) transfers its enhanced Node Base-station (eNB) with some information such as the Rank Indicator (RI) and Channel Quality Indicator (CQI) in order for the eNB to determine the most appropriate precoding matrix for transmitting the DL signals to multiple UEs with as little as possible interference among the UEs. In the procedure determining the precoding matrix at eNB, it can never be overemphasized that the information feed-back by each of the UEs should be as accurate as possible, meaning that the feedback information, (i.e., the RI and CQI), must reflect the real channel between eNB and each of the UEs accurately because the precoding matrix, which seriously affects the performance of a given MU-MIMO system, is obtained based on this information.

In this paper, we first explain how to select the most appropriate precoding technologies depending upon a given channel situation in an adaptive manner. The proposed procedure is applied to a test-bed system that has been implemented using a Graphic Processing Unit (GPU) and Universal Software Radio Peripheral (USRP) as an LTE-A modem and RF transceiver, respectively. Since the GPU includes a large number of cores, it is advantageous to reduce the processing time using parallel processing with the multiple cores [8].

II. TEST-BED MODEM ARCHITECTURE WITH PRECODER

In this section, the modem architecture of a non-codebook based 4x4 MU-MIMO system for TDD LTE-A [9] is introduced. As the system includes the dynamic precoding algorithm, we have implemented a test-bed of the 4X4 MU-MIMO system for verifying the performance of the proposed dynamic precoder.

A. Dynamic Precoder

As mentioned earlier, an MU-MIMO system in general employs a precoding procedure to mitigate interference among the signals transmitted from an eNB to multiple UEs. In this section, we introduce a novel MU-MIMO system for selecting the most appropriate precoding from a given set of precoders. For simplicity but without loss of generality, we consider two well-known precoding algorithms: Zero Forcing (ZF) and Lattice Reduction (LR) [10].

Figure 1 illustrates the BER performance of ZF and LR precoding method as a function of SNR when the number of antennas for both Tx and Rx is 4. It can be observed that the LR provides about 6dB improvement in SNR for BER = 10^{-3} compared to ZF.

978-1-5090-5932-4/17/$31.00 ©2017 IEEE

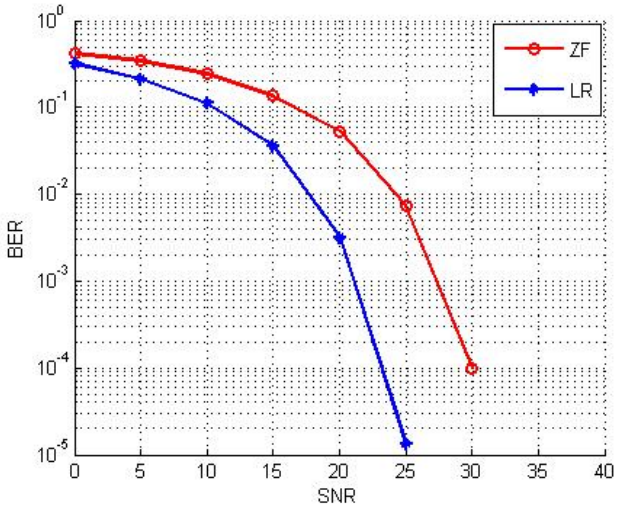

Fig. 1. Comparison of the BER performances (LR, ZF) when the number of antennas for both Tx and Rx is 4.

Summarizing the characteristics of each precoding method introduced above, we now propose a procedure for dynamically selecting a better appropriate precoding technology out of the two precoding methods depending upon the given signal environment. The parameter we consider to determine the better appropriate precoding is the Rx signal power, which reflects the Rx Signal to Noise Ratio (SNR) at each UE.

Figure 2 illustrates a flow chart for a dynamic precoding. For simplicity, but without loss of generality, let's first assume the upper bound for the BER has been set to be 10^{-3} and initially the precoding algorithm is set to be ZF because it is much simpler than LR. Then, since Figure 1 indicates that the BER becomes larger than 10^{-3} for SNR < about 27.5dB in the case of the ZF, the precoding algorithm should be switched from ZF

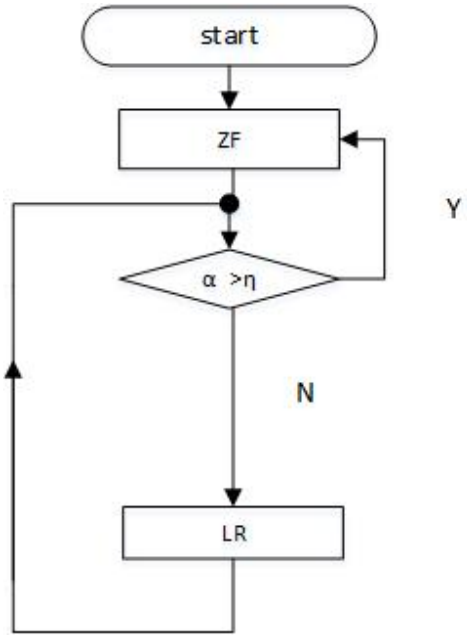

Fig. 2. Flow chart for a dynamic precoding

to LR when the SNR becomes lower than about 27.5dB. Recalling that the Rx signal power at the target UE determines the SNR, we first measure the Rx signal power at the target UE. In order to measure the Rx signal power at each UE, a reference signal of a unit magnitude that is known to both eNB and UE is transferred from the eNB encoder to a target Rx UE through the RF transceivers and antennas. Then, the decoder of the target UE measures the magnitude of the Rx reference signal to find the propagation path gain, α, shown in Figure 2. Note that α can be obtained easily by measuring it for an arbitrarily selected single subcarrier. In other words, as long as all the devices composing of the MU-MIMO system such as antennas and RF transceivers guarantees the linear phase characteristic within the entire frequency band, α should be approximately the same for all the subcarrier values of the LTE-A. Furthermore, since the reference signal of the unit magnitude is sent and received at the encoder and decoder, i.e., in the digital domain, of the Tx eNB and Rx UE, respectively, the measuring procedure is not at all complicated. Consequently, it has been empirically found through our experimental tests from our test-bed system (of which the details about implementation is shown in Section III) that the threshold value for α that determines the upper bound for BER, (i.e., 10^{-3}) is about 0.25. It should be noted that the threshold value for α might be different depending upon the desired upper bound of BER and other factors such as the thermal noise of the implemented system, which means that η should be determined empirically through experimental tests for a given MU-MIMO system.

B. Modem Architecture

In this sub-section, we introduce the modem architecture of 4X4 TDD MU-MIMO system which adopts the dynamic precoder shown in the previous sub-section. Since the MU-MIMO transmission is provided in DL, we have considered the frame type 2 with DL configuration 5 of 3 GPP Release 10 [11] in which the DL sub-frame takes 80% of the entire data frame. Meanwhile, Single-User MIMO instead of MU-MIMO has been adopted for the UL of our test-bed system for the purpose of stable feedback of the DL channel information.

Figure 3 illustrates the functional block diagrams of the modem implemented with GPUs for both DL and UL. The DL modem includes encoding eNB as shown in the upper part of Figure 3. Similarly, the UL modem includes decoding eNB as shown in the lower part of Figure 3.

The functional blocks for both DL and UL shown in Figure 3 are coincident with Release 10 except for the dynamic precoding that is included in the encoding part of the DL blocks shown at the top left-hand side of Figure 3. The precoder receives not only the modulated signals but also the control signals such as α, which represent the Rx signal power. The functional block shown as "dynamic precoding" in Figure 3 selects the better appropriate precoding algorithm between the given two, (i.e., ZF and LR).

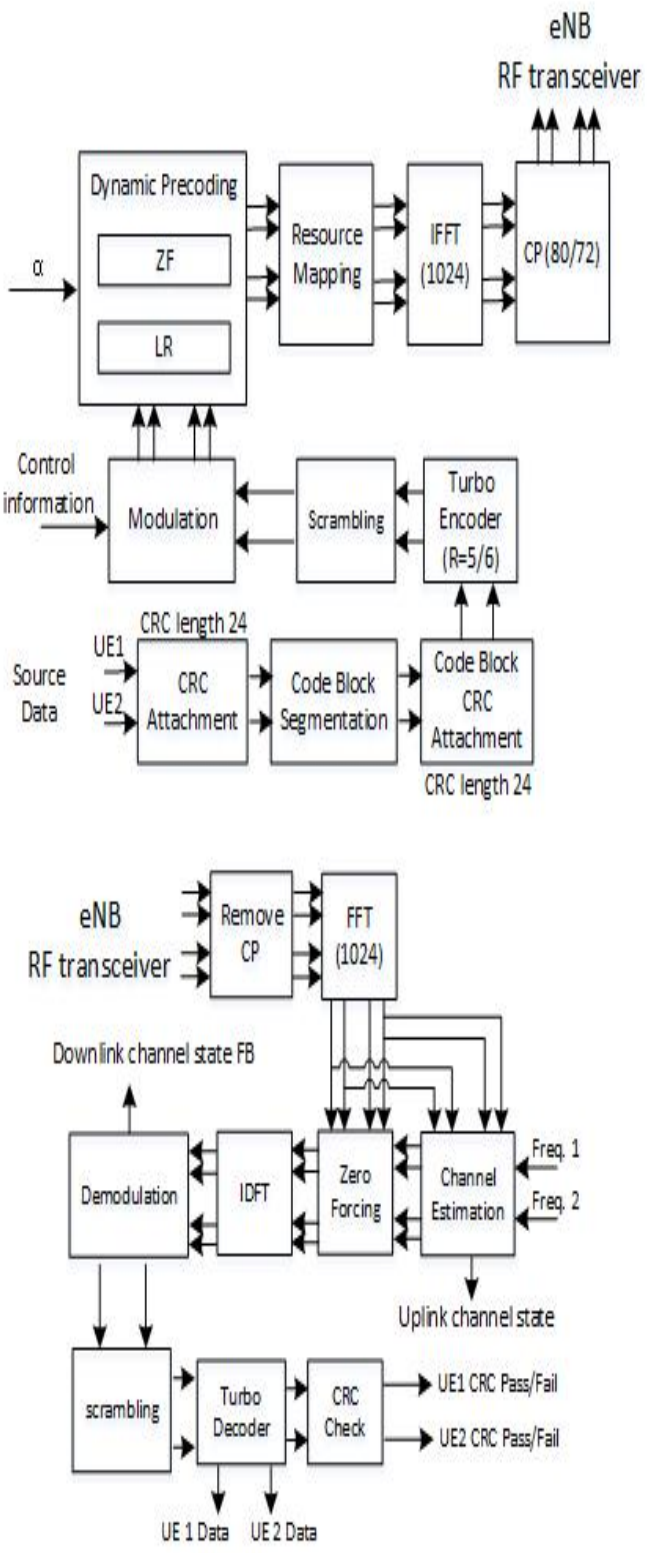

Fig. 3. Functional block diagram for DL modem and UL modem: encoding eNB and decoding eNB are shown in upper and lower part, respectively.

The parameters adopted in the implemented test-bed are summarized in Table 1.

Table 1 System parameters

Parameters	eNB	User Equipment
Number of Antennas	4	2 at each UE
Precoding	ZF/LR	Not Applicable
Waveform	3GPP Release 10	
FEC	Turbo coding, R=5/6	
FFT size	1024	
Modulation scheme	64QAM(PDSCH, PUSCH) QPSK(PDCCH, PUCCH)	
Center frequency	2.63Ghz	
Bandwidth	10Mhz	

III. System Implementation

This section presents the implementation of the 4X4 MU-MIMO test-bed system based on the modem architecture introduced in Section 2. The test-bed consists of a 4-antenna eNB and 2 of 2-antenna UEs.

Figure 4(a) and (b) illustrates a block diagram of eNB and UE, respectively. The modem part of which the architecture is introduced in Section 2 has been implemented with NVIDIA's GeForce GTX 780 Ti GPU, while USRP N210 [12] was used as an RF transceiver, for both eNB and UEs. The GPU-based modem [13, 14] is compliant to the Release 10 specifications. As shown in Figure 4, we adopted two GPUs, one for Rx and the other for Tx, for eNB and each UE. The gigabit Ethernet (GbE) shown in Figure 4 connects each transceiver to the Central Processing Unit (CPU) which has been used for controlling the GPU modem and RF transceiver. In order to separate the Tx and Rx paths, an off-the-shelf circulator was adopted for each antenna path of both eNB and UE. As will be discussed later in this section, a standard Personal Computer (PC) equipped with a CPU and multi-GPUs was utilized as the main body of both eNB and UE.

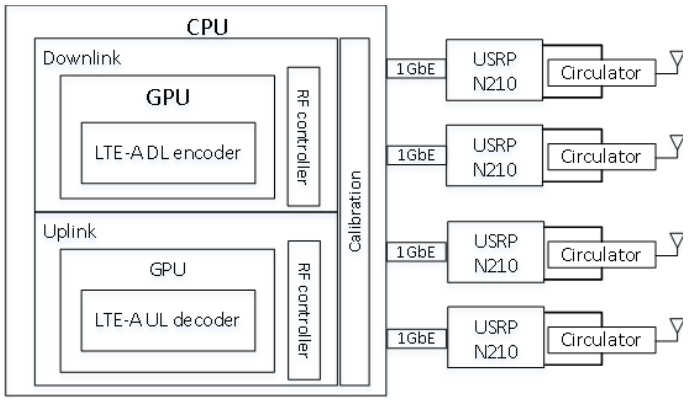

Fig. 4(a) System block diagram of eNB

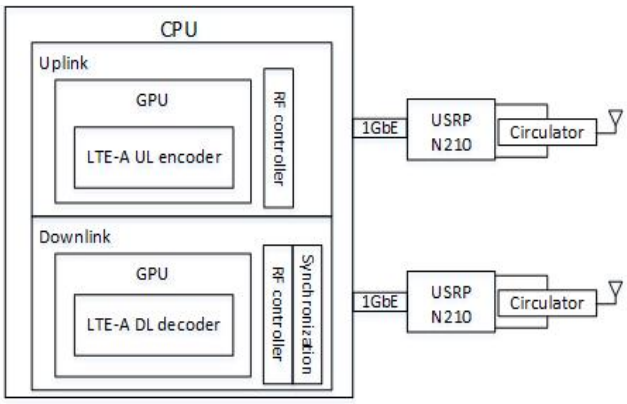

Fig. 4(b) System block diagram of UE

Fig. 4 System block diagram of eNB and UE

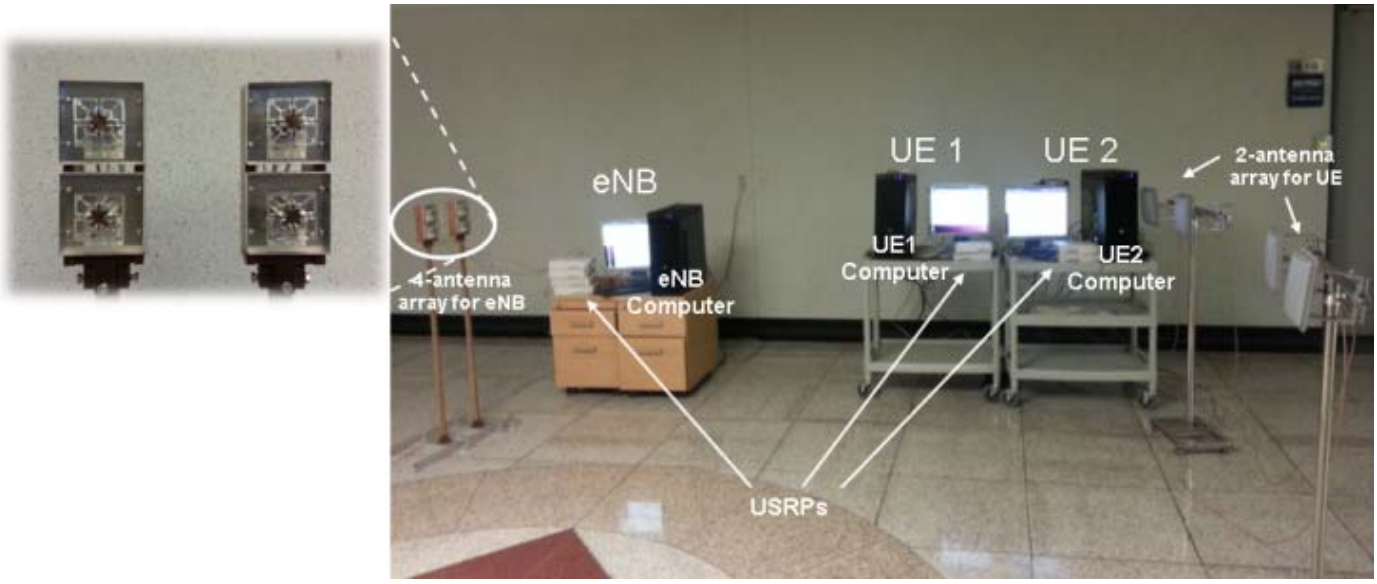

Fig. 5. Photograph of the Implemented 4x4 MU-MIMO Test-bed

Figure 5 illustrates a photograph of the implemented 4x4 MU-MIMO system test-bed consisting of a 4-antenna eNB and two 2-antenna UEs.

IV. NEMERICAL RESULTS

In this section, we present a performance analysis of the proposed MU-MIMO system using numerical results obtained from both computer simulations and experimental tests with the parameters shown in Table 1. For the analysis, we considered the following scenario: the distance between eNB and each UE increases causing the Rx signal power to decrease. As shown in Figure 5, experimental tests were performed with a Line-of-Sight indoor signal environment between eNB and each UE. As for the Tx signal power at eNB, the Tx power at eNB was set to be about 5dBm on average.

Figure 6 illustrates the BER performance provided by ZF and LR as a function of the distance between eNB and UEs according to the above-explained preset. UEs are moving further from the initial position where the distance from eNB is about 5 m. In order to observe the effect of SNR changes only, excluding the effect of highly correlated DL channels between the two UEs, the distance between the two UEs was set up to be no less than 2 m, which was determined to be far enough away from each other for the correlation between the two DL channels to be less than 0.1. As shown in Figure 6, the precoder first starts with ZF because the SNRs at the two UEs are initially low enough for the resultant BER to be lower than the preset upper bound, i.e., 10^{-3}. As the 2 UEs move away further from eNB, since ZF cannot provide the preset BER upper bound, i.e., 10^{-3}, the precoder should switch from ZF to LR at a position where the distance from eNB becomes about 7 m. The MU-MIMO system which employs LR can now tolerate it until the distance from eNB becomes about 13meters where the BER becomes about the upper limit, i.e., 10^{-3}. If the two UEs go any further than that distance, (i.e., about 13 m) the MU-MIMO system cannot provide a BER

lower than 10^{-3}, which means the system cannot operate as an MU-MIMO with the BER upper bound being 10^{-3}. Consequently, it can be concluded from this experiment that the relative SNR gain of 6dB provided by LR in comparison to ZF, as shown in Figure 1, contributes for the system to tolerate for about 6 (=13-7) meters of additional distance from eNB. Conversely speaking, when the UEs are located close enough from eNB, say, within 7 m, the system guarantees that the BER is lower than the preset upper bound, (i.e., 10^{-3}) even with a simple beamforming precoder, ZF, instead of such expensive precoders as LR.

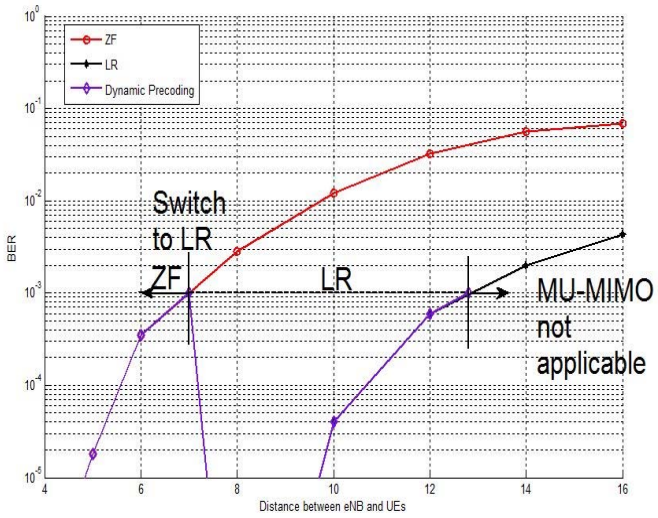

Fig. 6. Dynamic precoding applied to BER curve in terms of the distance between eNB and UE.

V. Conclusion

This paper presents an implementation of a 4x4 MU-MIMO test-bed system that operates in TDD LTE-A. The modem and RF transceiver of the test-bed were implemented with GPUs and USRPs, respectively, while the system control was performed by a CPU provided in a PC. The implemented system was utilized for verifying the performance of a proposed dynamic precoder in this paper. Using the dynamic precoder, one can select the most appropriate precoding technique among a given set depending upon the given signal environments. In this paper, we considered two precoding procedures, ZF and LR, to select from. From our experiments, it has been found that the maximum distance between eNB and each UE is about 13 m for the MU-MIMO system to guarantee the BER $<10^{-3}$ when the Tx power was set to about 5 dBm. It was found from our experiments that the implemented MU-MIMO system can provide BER $<10^{-3}$ using the proposed MU-MIMO system, which switches from ZF to LR. From various numerical results obtained from computer simulations and real experimental tests, we can conclude that the proposed dynamic precoding technology can enhance the performance with a minimum amount of computational burden.

Acknowledgment

"This work was supported by Institute for Information & communications Technology Promotion(IITP) grant funded by the Korea government(Ministry of Science, ICT&Future Planning, MSIP) (No.B0115-16-0001, 5G Communication with a Heterogeneous, Agile Mobile network in the PyeongChang wInter Olympic competioN). It was also supported by the MSIP, Korea, under the ITRC(Information Technology Research Center) support program (IITP-2016-H8501-16-1006) supervised by the IITP."

References

[1] Lingjia Liu; Runhua Chen; Geirhofer, S.; Sayana, K.; Zhihua Shi; Yongxing Zhou, "Downlink MIMO in LTE-advanced: SU-MIMO vs. MU-MIMO," *Communications Magazine, IEEE* , vol.50, no.2, pp.140,147, February 2012

[2] Ivrlac, M.T.; Choi, R.L.U.; Murch, R.D.; Nossek, J.A., "Effective use of long-term transmit channel state information in multi-user MIMO communication systems," *Vehicular Technology Conference, 2003. VTC 2003-Fall. 2003 IEEE 58th* , vol.1, no., pp.373,377 Vol.1, 6-9 Oct. 2003

[3] Kyunghoon Kim, Hyunwook Yang, Seungwon Choi, "User Selection Method Adopting Cross-Entropy Method for a Downlink Multiuser MIMO System", *Wireless Personal Communications*, Vol. 74, no. 2, pp.789-802, Jauary, 2014

[4] Chao Dong; Youzheng Wang; Jianhua Lu, "A Two-Step User Selection Algorithm for Multiuser Precoding," *Vehicular Technology, IEEE Transactions on* , vol.63, no.4, pp.1922,1927, May 2014

[5] Donghyun Kum, Daegeun Kang, and Seungwon Choi, "Novel SINR-Based User Selection for an MU-MIMO System with Limited Feedback," *ETRI Journal*, vol. 36, no. 1, Feb. 2014, pp. 62-68.

[6] Hyunwook Yang, Seungwon Choi, "MU-MIMO Precoding Methods for Reducing the Transmit Normalization Factor by Perturbing Data of the Codebook", *IEICE Transactions on Connunications*, Vol. E95.B, no. 7, pp. 2405-2413, 2012

[7] Hyunwook Yang, Taehyun Kim, Chiyung Ahn, June Kim, Seungwon Choi, John Glossner, "Implementation of parallel lattice reduction-aided MIMO detector using graphics processing unit", *Analog Integrated Circuits and Signal Processing*, Vol. 73, no. 2, pp 559-567, Nov. 2012

[8] NVIDIA. NVIDIA CUDA Programming Guide-2.2, 2009. http://developer. download.nvidia.com/compute/cuda/2-2/ toolkit/docs/NVIDIA-CUDA-Programming- Guide-2.2.pdf.

[9] 3GPP, 3GPP Keywords & Acronyms, "http://www.3gpp.org/technologies/keywords-acronyms/97-lte-advanced", June, 2013.

[10] Xiaoping Zhou; Xingliang Yin; Wenbo Wang, "Lattice Reduction Aided Precoding Mechanism for MIMO Systems," inWireless Communications, Networking and Mobile Computing (WiCOM), 2011 7th International Conference on , vol., no., pp.1-5, 23-25 Sept. 2011

[11] 3GPP TS 36.211, "Evolved Universal Terrestrial Radio Access(E-UTRA);Physical channels and modulation"

[12] Ettus Research, http://www.ettus.com/content/files/07495_Ettus_N200-210_DS_Flyer_HR_1.pdf.

[13] Chiyoung Ahn, June Kim, Jaehyuk Ju, Jinho Choi, Byungcho Choi, Seungwon Choi, "Implementation of an SDR platform Using GPU and its application to 2x2 MIMO Wimax system", *Analog Integrated Circuits and Signal Processing*, Vol.69, no. 2-3, pp.107-117, Dec, 2011

[14] Chiyoung Ahn, Saehee Bang, Hyohan Kim, Seunghak Lee, June Kim, Seungwon Choi, "Implementation of an SDR system Using an MPIbased GPU cluster for Wimax and LTE", *Analog Integrated Circuits and Signal Processing*, Vol. 73, no. 2, pp.569-582, Nov. 2012